JOURNAL OF SOLID STATE CHEMISTRY 118, 33–42 (1995)

Crystal Structure of $Na_7Fe_4(AsO_4)_6$ and α-$Na_3Al_2(AsO_4)_3$, Two Sodium Ion Conductors Structurally Related to II-$Na_3Fe_2(AsO_4)_3$

C. Masquelier,* F. d'Yvoire,*,[1] and G. Collin†

*Laboratoire de Chimie des Solides, URA CNRS 446, Université Paris-Sud, 91405 Orsay Cédex, France; and †Laboratoire Léon Brillouin, CE Saclay, Bâtiment, 563, 91191 Gif sur Yvette Cédex, France

Received August 1, 1994; in revised form January 9, 1995; accepted January 10, 1995

In the system Na_2O–Fe_2O_3–FeO–As_2O_5, $Na_7Fe_4(AsO_4)_6$ is one of the end members of a large domain of nonstoichiometry, including the sodium ion conductor II-$Na_3Fe_2(AsO_4)_3$. It is rhombohedral, space group $R\bar{3}c$, with cell constants a = 13.807(1) and c = 18.354(3) Å, and Z = 6. The structure is closely related to that of II-$Na_3Fe_2(AsO_4)_3$ and differs from it by a partial reduction of Fe^{III} into Fe^{II}, associated with an increase in sodium content for charge compensation; the reduction is localized on the Fe(1) site, and the Na(2) site is totally occupied, so that the structural formula can be written as $Na(1)Na(2)_6Fe^{II}(1)Fe^{III}(2)_3(AsO_4)_6$. $Na_3Al_2(AsO_4)_3$ undergoes at 44°C a reversible phase transition $\alpha \rightleftharpoons \beta$. The β form is rhombohedral and isotypic with II-$Na_3Fe_2(AsO_4)_3$. The room-temperature form, α, differs from β by a slight monoclinic distortion: a = 14.551(2), b = 13.303(1), c = 9.782(1) Å, β = 96.88(1)°, space group $C2$, and Z = 8. The sodium ions exhibit a long-range ordering: among the six available sodium sites derived from the Na(2) site of the β form, five are totally occupied and one is vacant. A comparison with the structure of II-$Na_3Fe_2(AsO_4)_3$ reveals some important displacements of Na positions toward the vacancy □(26), which probably result in a minimization of electrostatic repulsions. A close examination of the framework distortions indicates that the loss of symmetry (β, rhombohedral → α, monoclinic) could be associated with a loss of the three-dimensional character of the conduction. © 1995 Academic Press, Inc.

INTRODUCTION

The arsenates $Na_3M_2(AsO_4)_3$ (M = Al, Ga, Cr, Fe) (1, 2) do not have the Nasicon structure which is adopted by the corresponding phosphates $Na_3M_2(PO_4)_3$ (M = Cr, Fe) (3–5). They exhibit two structural modifications and, for $Na_3Fe_2(AsO_4)_3$, the ionic conductivity of the high-temperature form (II, rhombohedral) was found to be three orders of magnitude higher than that of the low-temperature form (I, garnet-type).

The crystal structure of II-$Na_3Fe_2(AsO_4)_3$ (6) consists of a three-dimensional framework $[Fe_4(AsO_4)_6]_\infty$ into which the sodium ions are inserted. The Na^+ ions are distributed over two sites: Na(1) and Na(2). Na(2) is partially occupied (occupancy factor τ = 5/6) and the structural formula is: $Na(1)Na(2)_5□Fe(1)Fe(2)_3(AsO_4)_6$.

Depending on the conditions of preparation, "nonstoichiometric" crystals can be obtained, which result from partial substitution of Na^+ and/or Fe^{2+} for Fe^{3+}. The compound $Na_7Fe_4(AsO_4)_6$ (i.e., $Na_7Fe^{II}Fe^{III}_3(AsO_4)_6$) is one of the end-members of the nonstoichiometric domain.

At 44°C $Na_3Al_2(AsO_4)_3$ undergoes a reversible phase transition $\alpha \rightleftharpoons \beta$, which was evidenced by DTA, conductivity measurements (Fig. 1), and X-ray powder diffraction. The high-temperature form β is rhombohedral, isotypic with II-$Na_3Fe_2(AsO_4)_3$. The room-temperature form α differs from β by a slight monoclinic distortion, which was assumed to be associated with a long-range ordering of the sodium ions (2).

In the present paper we report the crystal structures of $Na_7Fe_4(AsO_4)_6$ and α-$Na_3Al_2(AsO_4)_3$. This work was undertaken in order to confirm and specify

(i) the mechanism of the nonstoichiometry observed in II-$Na_3Fe_2(AsO_4)_3$;

(ii) the long-range ordering of the Na^+ ions in α-$Na_3Al_2(AsO_4)_3$. The positions of the sodium sites are examined as well as the atomic displacements associated with the distortion of the framework; then, models of conduction paths are discussed.

EXPERIMENTAL

Synthesis and Characterization

Crystals of II-$Na_7Fe_4(AsO_4)_6$ were grown in a flux of sodium arsenate from the starting mixture 13 Fe_2O_3 + 21 $Na_4As_2O_7$ + 24 $NaH_2AsO_4 \cdot H_2O$. After a progressive heating to 840°C, the mixture was melted at 1025°C, cooled to 500°C at a rate of 5°C · min^{-1} and then to room temperature (15°C · min^{-1}), with the melting and cooling operations being carried out in a flow of N_2. The crystals

[1] To whom correspondence should be addressed.

0022-4596/95 $12.00
Copyright © 1995 by Academic Press, Inc.
All rights of reproduction in any form reserved.

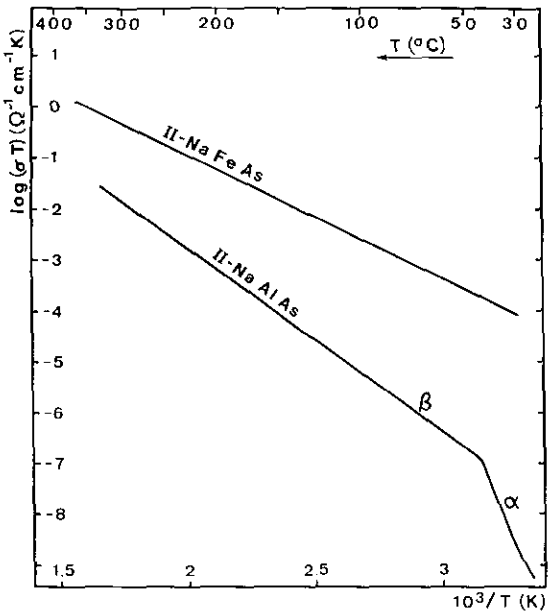

FIG. 1. Temperature dependence of the conductivity (σ) of II-$Na_3Fe_2(AsO_4)_3$ and $Na_3Al_2(AsO_4)_3$ (2).

obtained after washing in water are darkish. Microscopic observations reveal them to be uniaxial negative and pleochroïc: brown yellowish along **c**, dark gray perpendicular to **c**. Chemical analyses led to Fe^{II} and (Fe^{II} + Fe^{III}) contents of 4.34 and 14.04%, respectively, corresponding to the formula $Na_{6.95}Fe^{II}_{0.95}Fe^{III}_{3.05}(AsO_4)_6$. The selected crystal had an irregular shape and was elongated approximately along [721].

Crystals of $Na_3Al_2(AsO_4)_3$ were also obtained by flux techniques. The starting mixture $2Al(OH)_3 + Na_4As_2O_7 + 4NaH_2AsO_4 \cdot H_2O$ was progressively heated and melted up to 765°C, cooled to 670°C at a rate of 2°C · min^{-1}, and then quenched. The resulting solid was mainly vitreous, but some crystals could be isolated after a prolonged immersion in water. Preliminary X-ray diffraction investigations by means of the Weissenberg and precession methods indicated that the selected crystal was slightly twinned with one or two secondary domains in which the twofold axis was oriented from that of the main domain by a 120° rotation about the threefold pseudorotation axis. The crystal was elongated on [010] and delimited by {11$\bar{1}$} and {100}.

X-ray powder diffractograms of $Na_7Fe_4(AsO_4)_6$, β-$Na_3Al_2(AsO_4)_3$, and α-$Na_3Al_2(AsO_4)_3$ are presented in Table 1; *d* values have been corrected using $Al_4(P_4O_{12})_3$ as an internal standard (7). The cell parameters refined from the diffractograms are reported in the Abstract. They differ slightly from the values calculated from single crystal measurements (Table 2), especially in the case of α-$Na_3Al_2(AsO_4)_3$.

Structure Determination

Intensities were collected on an automatic four-circle diffractometer, using Mo$K\alpha$ radiation. Crystal data and experimental conditions for intensity measurements and refinements are reported in Table 2. Atomic scattering factors and anomalous dispersion corrections were taken from (11). The programs used have been developed locally from classical ones.

(*a*) $Na_7Fe_4(AsO_4)_6$. The structure of the isotypic compound II-$Na_3Fe_2(AsO_4)_3$ was used as a starting model. Atomic coordinates and anisotropic thermal motion coefficients were refined in the space group $R\bar{3}c$. Anharmonic corrections were applied to As and Na by using doubly contracted (instead of third- and fourth-rank) tensors. The occupancy factors, τ, of the Na(2) and Fe(2) sites were refined and found to be very close to 1 (then fixed at 1 for Fe(2)). The final *R* values are $R = 4.87\%$ and $R_w = 5.75\%$. Final atomic parameters are listed in Table 3. Selected interatomic distances and angles are given in Table 4.[2]

(*b*) α-$Na_3Al_2(AsO_4)_3$. Weissenberg and precession photographs indicate the presence of weak reflections *h*0*l* with $l = 2n + 1$. (Particularly worth noting is the fact that reflections $\bar{2}l0l$ with $l = 2n + 1$ are clearly observed: they are equivalent to reflections 00.3*l* in the pseudohexagonal cell and their presence on the photographs cannot be interpreted as a consequence of the twinning.) Then the unique reflection condition is *hkl*: $h + k = 2n$. Of the three possible space groups *C*2, *Cm*, and *C*2/*m*, only *C*2 is a subgroup of $R\bar{3}c$, the space group of the β form.

The atomic coordinates (x_h, y_h, z_h) of II-$Na_3Fe_2(AsO_4)_3$ (rhombohedral, hexagonal unit-cell) were transformed into (x_m, y_m, z_m) (monoclinic description) according to the relationships indicated in Fig. 2.

In the first stage, refinements were performed in the space group *C*2/*c* as an intermediate fictitious solution. Thus, any site A(*n*) in general position in the space group $R\bar{3}c$ was split into three independent sites, A(*n*1), A(*n*2), and A(*n*3), in the space group *C*2/*c* (Table 5). The occupancy factors, τ, of the Na(21), Na(22), and Na(23) sites were refined and found to be equal to 1, 1, and 0.5, respectively.

Then the structure was solved in the space group *C*2, which differs from *C*2/*c* by the loss of the inversion center. Any site A(*np*) ($p = 1$, 2, or 3) in general position in *C*2/*c* generates two sites: A(*np*) and A($n(p + 3)$). The Na(23) site was found to be totally occupied in *C*2 while the Na(26) site was vacant. At this step, refinements led to an *R* value of 9.8%. A significant improvement occurred

[2] Lists of structure factors and anisotropic thermal motion parameters are available upon request from the authors.

TABLE 1
X-Ray Powder Diffraction Data[a]

$Na_7Fe_4(AsO_4)_6$

I_c	d_{obs}/Å	d_{cal}/Å	h k.*l*
55	7.282	7.280	0 1.2
2	6.910	6.903	1 1.0
28	4.576	4.579	1 1.3
15	4.388	4.388	2 1.1
1	4.283	4.284	1 0.4
9	4.055	4.054	1 2.2
3	3.984	3.986	3 0.0
1	3.641	3.640	0 2.4
26	3.451	3.452	2 2.0
5	3.263	3.263	1 3.1
22	3.220	3.220	2 1.4
5	3.118	3.119	3 1.2
4	3.059	3.059	0 0.6
23	3.006	3.006	2 2.3
100	2.8493	2.8493	1 2.5
5	2.8430	2.8423	0 4.2
15	2.7130	2.7130	3 2.1
10	2.6885	2.6878	1 3.4
45	2.6093	2.6093	4 1.0
1	2.5040	2.5047	4 0.4
17	2.4610	2.4608	3 1.5

β-$Na_3Al_2(AsO_4)_3$ (50°C)

I_e	d_{obs}/Å	d_{cal}/Å	h k.*l*
40	7.205	7.200	0 1.2
3	6.643	6.640	1 1.0
20	4.514	4.514	1 1.3
8	4.284	4.284	1 0.4
45	4.233	4.232	2 1.1
10	3.933	3.933	1 2.2
6	3.834	3.834	3 0.0
2	3.600	3.600	0 2.4
30	3.321	3.320	2 2.0
25	3.165	3.165	2 1.4
15	3.144	3.143	1 3.1
15	3.078	3.078	0 0.6
4	3.015	3.015	3 1.2
20	2.9220	2.9223	2 2.3
100	2.8153	2.8147	1 2.5
8	2.6243	2.6244	1 3.4
12	2.6118	2.6121	3 2.1
20	2.5101	2.5099	4 1.0
4	2.4405	2.4407	4 0.4
10	2.4143	2.4142	3 1.5

α-$Na_3Al_2(AsO_4)_3$

I_c	d_{obs}/Å	d_{cal}/Å	h k *l*	h'k'.*l'*
42	7.224	7.223	2 0 0	0 1 .2
67	7.190	7.191	-1 1 1	
7	6.636	6.651	0 2 0	1 1 .0
		6.630	1 1 1	
37	4.525	4.528	3 1 0	1 1 .3
		4.520	-2 2 1	
14	4.498	4.497	-1 1 2	
18	4.293	4.293	-3 1 1	1 0 .4
6		4.274	-2 0 2	
100	4.236	4.239	1 3 0	2 1 .1
		4.234	2 2 1	
40	4.216	4.216	1 1 2	
24	3.937	3.937	3 1 1	1 2 .2
		3.936	-1 3 1	
11	3.922	3.922	0 2 2	
13	3.836	3.836	1 3 1	3 0 .0
4	3.826	3.823	2 0 2	
1		3.612	4 0 0	0 2 .4
3	3.597	3.596	-2 2 2	
25	3.3256	3.3257	0 4 0	2 2 .0
52	3.3154	3.3148	2 2 2	
52	3.1731	3.1739	4 2 0	2 1 .4
		3.1708	-3 3 1	
42	3.1492	3.1506	-1 1 3	
		3.1464	0 4 1	
27	3.1403	3.1398	3 1 2	1 3 .1
		3.1392	1 3 2	
40	3.0801	3.0799	-4 0 2	0 0 .6
5	3.0205	3.0209	2 4 0	3 1 .2
		3.0191	3 3 1	
4	3.0016	3.0016	1 1 3	
35	2.9264	2.9272	4 2 1	2 2 .3
		2.9265	-2 4 1	
21	2.9108	2.9108	0 2 3	
93	2.8237	2.8234	5 1 0	1 2 .5
91	2.8160	2.8155	-3 3 2	
86	2.8070	2.8066	-2 2 3	
8	2.6293	2.6299	5 1 1	1 3 .4
5	2.6244	2.6247	-2 4 2	
21	2.6172	2.6176	-1 3 3	
		2.6166	1 5 0	
11	2.6113	2.6114	3 3 2	3 2 .1
13	2.6044	2.6043	2 2 3	
25	2.5125	2.5128	1 5 1	4 1 .0
26	2.5085	2.5093	2 4 2	
25	2.5034	2.5034	3 1 3	

[a] Guinier camera, Co$K\alpha_1$ radiation. The intensities listed are either estimated visually (I_e) or calculated from single crystal data (I_c). For α-$Na_3Al_2(AsO_4)_3$, *h*, *k*, *l* and *h'*, *k'*, *l'* are the indices expressed with respect to the monoclinic and the pseudohexagonal cell, respectively. For β-$Na_3Al_2(AsO_4)_3$, a_h = 13.281(2) Å and c_h = 18.467(3) Å (2).

when taking into account the slight twinning mentioned above. The relative proportions of the three twin components were refined and found to be equal to 88, 7, and 5%. Anisotropic thermal motion factors were refined for the Na and As sites only. For the oxygen sites, the temperature factors $B(A(np))$ and $B(A(n(p + 3)))$ were constrained to be equal. The final R values are R = 4.13% and R_w = 4.71%. Final atomic parameters are listed in Table 6. Selected interatomic distances and angles are given in Tables 7 and 8.[2]

STRUCTURE OF II-$Na_3Fe_2(AsO_4)_3$

The main features of the crystal structure of II-$Na_3Fe_2(AsO_4)_3$ (6) are reported here and will serve as a reference for the following descriptions.

TABLE 2
Crystal Data and Experimental Conditions for Crystallographic Analysis of $Na_7Fe_4(AsO_4)_6$ and α-$Na_3Al_2(AsO_4)_3$

	$Na_7Fe_4(AsO_4)_6$	α-$Na_3Al_2(AsO_4)_3$
Crystal data		
Crystal system	Rhombohedral	Monoclinic
Space group	$R\bar{3}c$	$C2$
a (Å)	13.794(4)	14.576(6)
b (Å)	13.794(4)	13.409(6)
c (Å)	18.360(6)	9.728(5)
β (°)	90	96.95(4)
γ (°)	120	90
V (Å^3)	3025(2)	1887(2)
Z	6	8
Formula mass (amu)	1217.8	539.7
Crystal size (mm)	0.3 × 0.15 × 0.10	0.19 × 0.16 × 0.04
Dx (g · cm^{-3})	4.01	3.80
μ(Mo$K\alpha$) (mm^{-1})	12.84	10.92
Intensity measurements		
Monochromator	Graphite	
λ(Mo$K\alpha$) (Å)	0.7107	
T (K)	294	
Scan mode	$\theta - 2\theta$	
θ Range (°)	2 – 32.5	
Refinements		
Number of reflections collected	1450	3696
Number of unique reflections	881 ($I \geq 1\sigma(I)$)	2688 ($I \geq 3\sigma(I)$)
Absorption corrections	Integration from crystal shape	
Refinement method	Full-matrix least-squares on F	
Weighting scheme	unitary	
Agreement factors	$R = 0.049$	$R = 0.041$
	$R_w = 0.057$	$R_w = 0.047$

The space group is $R\bar{3}c$. A three-dimensional framework $[Fe_4(AsO_4)_6]_\infty$, made up of Fe_4O_{18} clusters linked to AsO_4 tetrahedra (Fig. 3), delimits an interstitial space within which the Na^+ ions are distributed.

Each Fe_4O_{18} cluster is built up of a central octahedron $Fe(1)O_6$ sharing three edges with $Fe(2)O_6$ octahedra. This arrangement probably results in some constraints around the Fe(1) site, since the Fe(1)–O(3) distance (1.987(5) Å) is significantly lower than the mean Fe(2)–O distance (2.016 Å).

Each tetrahedron shares two oxygens, O(1) and O(3), with one cluster and one oxygen, O(2), with another cluster. The fourth oxygen, O(4), belongs to the tetrahedron only and lies in the environment of the sodium ions. The As–O(4) distance is the shortest one (1.634(6) Å) and O(4) displays a high equivalent isotropic temperature factor (1.8(2) Å^2).

The sodium ions are distributed over two sites and are partially disordered: Na(1) is fully occupied and octahedrally surrounded ($\bar{3}$ symmetry) by the oxygen O(4) with a Na–O distance of 2.375(6) Å. Na(2) is partially occupied ($\tau = 5/6$) and has an irregular environment of nine oxygen atoms, with Na–O distances ranging from 2.29 to 3.12 Å. The Na(1) site is surrounded by a sextuplet of Na(2) equivalent positions. Each Na(2) position has two neighboring Na(2) positions belonging to the same sextuplet and one neighboring Na(2) position belonging to another

TABLE 3
Occupancy Factors, Atomic Coordinates, and Isotropic Temperature Factors of II-$Na_7Fe_4(AsO_4)_6$

Atom	Occupancy	x	y	z	B_{eq} (Å^2)[a]
Na(1)	1	0	0	0	1.31(22)
Na(2)	0.98(2)	0.7915(4)	0.0166(4)	0.0537(2)	1.74(15)
Fe(1)	1	0	0	1/4	0.59(7)
Fe(2)	1	0.7804(1)	0	1/4	0.47(6)
As	1	0.18456(6)	−0.01130(6)	0.14550(5)	0.56(2)
O(1)	1	0.5279(5)	0.0620(5)	0.1472(3)	0.97(18)
O(2)	1	0.7130(5)	0.0545(5)	0.1781(3)	1.00(19)
O(3)	1	0.5924(5)	0.1874(5)	0.0210(3)	0.88(17)
O(4)	1	0.0251(6)	0.1644(6)	0.0608(3)	1.14(19)

[a] $B_{eq} = (8/3)\pi^2 \Sigma_i \Sigma_j U_{ij} a_i^* a_j^* \mathbf{a}_i \cdot \mathbf{a}_j$.

TABLE 4
Selected Interatomic Distances (Å) and Angles (°) in $Na_7Fe_4(AsO_4)_6$

AsO_4 tetrahedron[a]

As	O(1)	O(2)	O(3)	O(4)
O(1)	1.704(6)	2.668(9)	2.851(9)	2.761(9)
O(2)	103.3(3)	1.698(7)	2.751(9)	2.833(9)
O(3)	113.5(3)	107.9(3)	1.704(6)	2.681(9)
O(4)	110.7(3)	115.5(3)	106.0(3)	1.651(7)

$Fe(1)O_6$ octahedron

Fe(1)–O(3)	×6	*2.086(6)*	*O(3)–Fe(1)–O(3')*	×3	*86.52(35)*
O(3)–O(3')	×1	2.86(1)	O(3)–Fe(1)–O(3'')	×3	87.96(37)
O(3)–O(3'')	×1	2.90(1)	O(3)–Fe(1)–O(3''')	×6	92.76(25)
O(3)–O(3''')	×1	3.02(1)	O(3)–Fe(1)–O(3'''')	×3	179.01(35)
O(3)–O(3'''')	×1	4.17(1)			

$Fe(2)O_6$ octahedron[a]

Fe(2)	O(2)	O(2)	O(1)	O(1)	O(3)	O(3)
O(2)	1.967(7)	2.94(1)	3.057(9)	2.699(9)	2.829(9)	4.03(1)
O(2)	96.8(4)	1.967(7)	1.980(6)	3.94(1)	2.758(8)	2.769(9)
O(1)	101.5(3)	86.3(3)	1.980(6)	3.94(1)	2.758(8)	2.769(9)
O(1)	86.3(3)	101.5(3)	168.4(4)	1.980(6)	2.769(9)	2.758(8)
O(3)	88.7(3)	170.9(3)	85.6(3)	86.0(3)	2.079(6)	2.86(1)
O(3)	170.9(3)	88.7(3)	86.0(3)	85.6(3)	86.9(4)	2.079(6)

NaO_n polyhedra

Na(1)–O(4)	×6	2.392(7)	Na(2)–O(2)	×1	2.688(8)
			Na(2)–O(4)	×1	2.827(9)
Na(2)–O(4)	×1	2.288(8)	Na(2)–O(1)	×1	3.019(8)
Na(2)–O(4)	×1	*2.514(9)*	*Na(2)–O(1)*	×1	*3.071(8)*
Na(2)–O(1)	×1	2.529(8)	Na(2)–O(3)	×1	2.940(8)
Na(2)–O(2)	×1	2.597(8)			

[a] As–O and Fe–O distances are underlined. The O–O distances are given above the diagonal, the O–As–O and O–Fe–O angles are given below.

sextuplet. After a close examination of the radius of the oxygen windows (i.e., the distance from the center of the window to the oxygen atoms lying at the corners) which separate neighboring sodium sites, d'Yvoire *et al.* (6) suggested two models of conduction paths (Fig. 3):

(a) ···Na(2)]–[Na(2)···Na(1)···Na(2)]–[Na(2)···Na(1)···
(b) ···Na(2)]–[Na(2)···Na(2)]–[Na(2)···

(The square brackets enclose Na positions belonging to, or centered inside, the same sextuplet.) These models have in common the ···Na(2)]–[Na(2)··· sequence, in which the Na(2) positions belong to different sextuplets and are separated by a wide quasirectangular window with R = 2.38 Å. In contrast, two neighboring Na positions Na(2)···Na(2) belonging to the same sextuplet as well as Na(2)···Na(1), are separated by narrow windows with R = 1.89 and R = 1.91 Å, respectively.

The high value of the temperature factor on the Na(2) site (B_{eq} = 3.98(26) Å^2) is in favor of the *b*-model but ion-exchange experiments, which lead to a quasi-total substitution of Ag^+ or Li^+ for Na^+, suggest that Na(1) might also be involved in the conduction process (*a*-model).

STRUCTURE OF $Na_7Fe_4(AsO_4)_6$

The structure, described in the space group $R\bar{3}c$, is very similar to that of II-$Na_3Fe_2(AsO_4)_3$ (called stoichiometric) but differs from it by three main specific features:

—*The occupancy factor of the Na(2) site is very close to* 1 (τ = 0.98(2)) while it is equal to 5/6 in the stoichiometric crystal. The quasitotal occupancy of the Na(2) site is accompanied by a significant decrease in the average Na(2)–O distance: 2.719 Å against 2.745 Å.

—The average Fe(2)–O distance (2.009 Å) is virtually the same as in the stoichiometric compound (2.016 Å) and can be considered as characteristic of iron in the oxidation state +3. The Fe(1) site is fully occupied in both compounds but the Fe(1)–O(3) distance is much longer in $Na_7Fe_4(AsO_4)_6$ (2.086(6) Å) than in II-$Na_3Fe_2(AsO_4)_3$ (1.987(5) Å). This difference of 0.10 Å suggests that, in $Na_7Fe_4(AsO_4)_6$, the Fe(1) site is occupied by iron in the oxidation state +2. Similar observations were reported

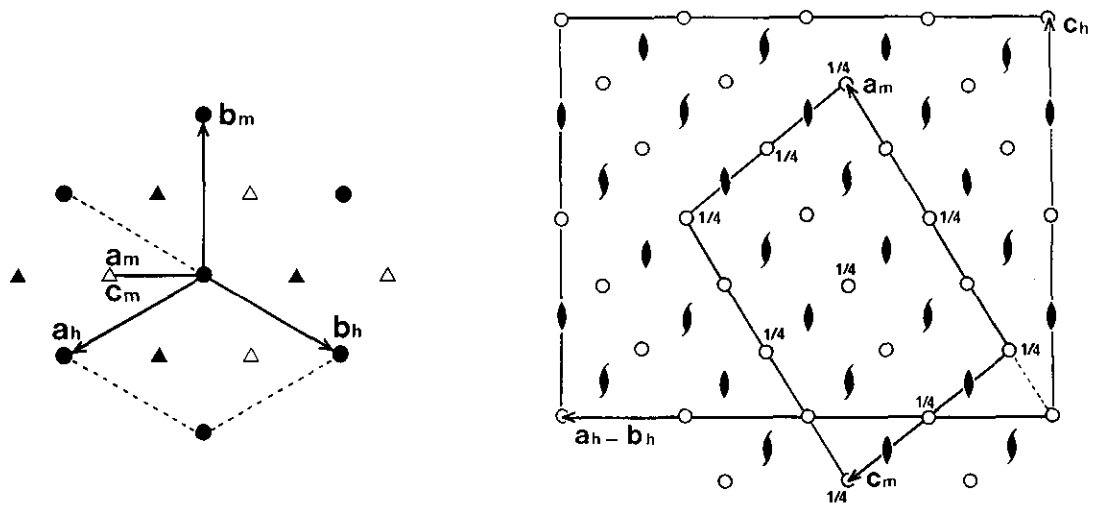

FIG. 2. Geometrical relationships between the hexagonal unit cell ($\mathbf{a}_h$, $\mathbf{b}_h$, $\mathbf{c}_h$) (space group $R\bar{3}c$) and the monoclinic unit cell ($\mathbf{a}_m$, $\mathbf{b}_m$, $\mathbf{c}_m$) of $Na_3Al_2(AsO_4)_3$:

$$\mathbf{a}_m = \mathbf{a}_h/3 - \mathbf{b}_h/3 + 2\mathbf{c}_h/3, \quad \mathbf{b}_m = -\mathbf{a}_h - \mathbf{b}_h, \quad \mathbf{c}_m = \mathbf{a}_h/3 - \mathbf{b}_h/3 - \mathbf{c}_h/3$$

Left, projection along $[001]_h$. Lattice points at $z_h = 0$, 1/3, and 2/3 are represented by full circles, full triangles, and open triangles, respectively. *Right*, projection along $[010]_m$. The space group considered here is $C2/c$, which corresponds to an intermediate fictitious solution. The atomic coordinates x_h, y_h, z_h of II-$Na_3Fe_2(AsO_4)_3$ (rhombohedral) were transformed into x_m, y_m, z_m (monoclinic) according to the following relationships: $x_m = (x_h - y_h)/2 + z_h - 1/4$, $y_m = -(x_h + y_h)/2 - 1/4$, and $z_m = x_h - y_h - z_h$. In order to be consistent with the description of the "International Tables of Crystallography," the origin was shifted by $(\mathbf{a}_m + \mathbf{b}_m)/4$. For the description in the $C2$ space group, it must be translated again by $\mathbf{c}_m/4$.

TABLE 5
Differentiation of the Na and Al Sites in the Space Groups $R\bar{3}c$, $C2/c$, and $C2$

β-$Na_3Al_2(AsO_4)_3$ Rhombohedral $R\bar{3}c$ $Z = 12$				$Na_3Al_2(AsO_4)_3$ Monoclinic $C2/c$ $Z = 8$				α-$Na_3Al_2(AsO_4)_3$ Monoclinic $C2$ $Z = 8$		
Site	Position	Symmetry	τ	Site	Position	Symmetry	τ	Site	Position	τ
Na(1)	6*b*	$\bar{3}$	1	Na(1)	4*c*	$\bar{1}$	1	Na(1)	4*c*	1
				Na(21)	8*f*	1	1	Na(21)	4*c*	1
								Na(24)	4*c*	1
Na(2)	36*f*	1	5/6	Na(22)	8*f*	1	1	Na(22)	4*c*	1
								Na(25)	4*c*	1
				Na(23)	8*f*	1	0.5	Na(23)	4*c*	1
								Na(26)	4*c*	0
Al(1)	6*a*	32	1	Al(1)	4*e*	2	1	Al(11)	2*b*	1
								Al(14)	2*a*	1
Al(2)	18*e*	2	1	Al(21)	4*e*	2	1	Al(21)	2*b*	1
								Al(24)	2*a*	1
				Al(22)	8*f*	1	1	Al(22)	4*c*	1
								Al(25)	4*c*	1

TABLE 6
Atomic Coordinates and Isotropic Temperature Factors of α-$Na_3Al_2(AsO_4)_3$

Atom	x	y	z	B(Å^2)[a]
Na(1)	0.2512(5)	0.751(1)	0.2378(8)	1.44(22)
Na(21)	0.1844(5)	0.544(1)	0.2673(7)	1.26(24)
Na(24)	0.7984(5)	0.499(1)	0.173(1)	2.39(26)
Na(22)	0.0998(6)	0.862(1)	0.075(1)	1.92(40)
Na(25)	0.9002(6)	0.132(1)	0.4092(9)	1.19(31)
Na(23)	0.8132(5)	0.359(1)	0.5166(8)	1.96(30)
Al(11)	0	0.750(1)	1/2	0.56(4)
Al(14)	0	0.250(1)	0	0.56(4)
Al(21)	0	0.529(1)	1/2	0.82(14)
Al(24)	0	0.469(1)	0	0.53(12)
Al(22)	0.3877(4)	0.357(1)	0.2805(6)	0.60(8)
Al(25)	0.6095(4)	0.638(1)	0.2229(6)	0.58(9)
As(11)	0.1938(1)	0.644(1)	0.5741(2)	0.60(6)
As(14)	0.8082(1)	0.348(1)	−0.0827(2)	0.57(6)
As(12)	0.4994(1)	0.162(1)	0.1990(2)	0.53(7)
As(15)	0.4933(1)	0.832(1)	0.2974(2)	0.58(7)
As(13)	0.1069(1)	0.934(1)	0.4053(2)	0.65(7)
As(16)	0.8923(1)	0.058(1)	0.0909(2)	0.53(6)
O(11)	0.1282(9)	0.542(2)	0.570(1)	0.76(9)
O(14)	0.8782(9)	0.451(2)	−0.087(1)	0.76(9)
O(12)	0.4156(9)	0.251(2)	0.169(1)	0.84(8)
O(15)	0.5762(9)	0.746(2)	0.336(1)	0.84(8)
O(13)	0.1302(9)	0.949(2)	0.577(1)	0.68(8)
O(16)	0.8728(9)	0.042(2)	−0.084(1)	0.68(8)
O(21)	0.0384(9)	0.435(2)	0.374(1)	0.71(9)
O(24)	0.9599(9)	0.551(2)	0.130(1)	0.71(9)
O(22)	0.9277(9)	0.946(2)	0.153(1)	0.72(9)
O(25)	0.0675(9)	0.050(2)	0.354(1)	0.72(9)
O(23)	0.7406(9)	0.360(2)	0.765(1)	0.84(9)
O(26)	0.2666(9)	0.640(2)	−0.280(1)	0.84(9)
O(31)	0.0221(9)	0.643(2)	0.378(1)	0.73(7)
O(34)	0.9760(9)	0.351(2)	0.119(1)	0.73(7)
O(32)	0.0187(9)	0.848(2)	0.369(1)	0.67(8)
O(35)	0.9814(9)	0.145(2)	0.126(1)	0.67(8)
O(33)	0.625(1)	0.249(2)	0.576(1)	0.60(8)
O(36)	0.376(1)	0.740(2)	−0.083(1)	0.60(8)
O(41)	0.2488(8)	0.655(2)	0.438(1)	0.91(10)
O(44)	0.7535(8)	0.356(2)	0.055(1)	0.91(10)
O(42)	0.601(1)	0.195(2)	0.152(1)	1.02(9)
O(45)	0.397(1)	0.796(2)	0.352(1)	1.02(9)
O(43)	0.196(1)	0.899(2)	0.326(1)	0.99(9)
O(46)	0.807(1)	0.101(2)	0.165(1)	0.99(9)

[a] Na and As atoms anisotropically refined: $B_{eq} = (8/3)\pi^2 \Sigma_i \Sigma_j U_{ij} a_i^* a_j^* \mathbf{a}_i \cdot \mathbf{a}_j$.

for mixed-valence Fe^{II}–Fe^{III} compounds (8, 9). The structural formula of the studied crystal can be written Na(1) $Na(2)_6Fe^{II}(1)Fe^{III}(2)_3(AsO_4)_6$ and the mechanism previously proposed (6) to account for the nonstoichiometry phenomenon is confirmed: a substitution of Fe^{2+} and/or Na^+ for Fe^{3+} occurs in the Fe(1) site and is compensated for by a higher occupancy of the Na(2) site for charge balance.

—The thermal motion factors are significantly lower in the nonstoichiometric crystal, especially on the Na(2) site. This suggests a decrease in ionic transport properties associated with the decrease of the vacancy/Na ratio within the interstitial space.

A confirmation of this point would require good conductivity measurements on single crystals or dense ceramic samples of appropriate size. As yet such samples have not been elaborated. Moreover, besides the ionic conduction, an electronic one could be induced by the presence of mixed valence Fe^{III}–Fe^{II} in the material.

STRUCTURE OF α-$Na_3Al_2(AsO_4)_3$

The structure of α-$Na_3Al_2(AsO_4)_3$, described in the space group $C2$, is characterized by a long-range ordering of the Na^+ ions. The phase transition between the high-temperature form β (isotypic with II-$Na_3Fe_2(AsO_4)_3$) and the α form adopted below 44°C is accompanied by a small monoclinic distortion, without any breaking or creating of interatomic bonds in the framework.

Sodium ion distribution. The arrangement of the sodium sites in α-$Na_3Al_2(AsO_4)_3$ is shown in Fig. 4, which clearly illustrates the loss of rhombohedral symmetry. The Na(1) site, fully occupied, is surrounded by six independent Na($2p$) sites (p = 1 to 6) among which five are totally occupied (Na(21) → Na(25)) and one is vacant (□(26)).

The Na–Na distances in α-$Na_3Al_2(AsO_4)_3$ were calculated. In Table 9, they are compared with the corresponding values obtained from the Na coordinates of II-$Na_3Fe_2(AsO_4)_3$ applied to the α-$Na_3Al_2(AsO_4)_3$ lattice. Important shifts of the three sodium sites Na(24), Na(21) and Na(22) toward the vacancy □(26) are observed: 0.55, 0.25, and 0.12 Å, respectively. This suggests that the ordering is associated with a minimization of electrostatic repulsions between neighboring Na^+ ions. A similar observation was recently reported for the ordered form α of $Na_7Fe_3(P_2O_7)_4$ (10). The other Na(2p)–Na(2p′) distances are slightly increased and the Na(1)–Na(2p) distances remain quite unchanged, except the Na(1)–Na(24) one, for which the increase (+0.40 Å) seems to be a direct consequence of the displacement of the Na(24) site toward the □(26) vacancy.

AsO_4 tetrahedra. There are six independent tetrahedra (Table 7) and the mean As–O distance (1.690 Å) is very close to that observed in II-$Na_3Fe_2(AsO_4)_3$ (1.688 Å).

AlO_6 octahedra. (Table 8). The central octahedra $Al(11)O_6$ and $Al(14)O_6$, which belong to the two crystallographically independent clusters Al_4O_{18}, are slightly distorted. In the other octahedra, the Al–O distances range from 1.83(1) to 2.03(2) Å. The shortest ones correspond to the oxygen atoms O(24), O(12), and O(26) which surround the sodium vacancy □(26). In both Al_4O_{18} clusters, the Al–O distances are significantly shorter in the central

TABLE 7
Interatomic Distances (Å) and Angles (°) in AsO_4 Tetrahedra of α-$Na_3Al_2(AsO_4)_3$

As(11)	O(41)	O(26)	O(11)	O(33)	As(14)	O(44)	O(23)	O(14)	O(36)
O(41)	1.63(1)	2.73(2)	2.76(2)	2.69(2)	O(44)	1.64(1)	2.80(2)	2.73(2)	2.82(2)
O(26)	111.6(6)	1.66(1)	2.68(2)	2.77(2)	O(23)	114.8(6)	1.68(1)	2.62(2)	2.82(2)
O(11)	113.2(6)	107.0(7)	1.67(1)	2.78(2)	O(14)	108.4(6)	101.0(6)	1.72(1)	2.83(2)
O(33)	106.0(7)	109.5(7)	109.6(6)	1.73(2)	O(36)	112.4(6)	110.4(7)	109.1(6)	1.76(2)
As(12)	O(42)	O(24)	O(12)	O(31)	As(15)	O(45)	O(21)	O(15)	O(34)
O(42)	1.66(1)	2.80(2)	2.83(2)	2.69(2)	O(45)	1.63(1)	2.76(2)	2.72(2)	2.76(2)
O(24)	112.8(6)	1.71(1)	2.79(2)	2.76(2)	O(21)	113.9(7)	1.66(1)	2.61(2)	2.76(2)
O(12)	114.6(8)	109.9(7)	1.71(1)	2.80(2)	O(15)	110.2(8)	103.7(7)	1.68(2)	2.80(2)
O(31)	104.2(7)	106.2(7)	108.6(7)	1.75(1)	O(34)	110.0(7)	109.2(8)	109.6(7)	1.74(1)
As(13)	O(43)	O(25)	O(13)	O(32)	As(16)	O(46)	O(22)	O(16)	O(35)
O(43)	1.65(1)	2.80(2)	2.81(2)	2.75(2)	O(46)	1.62(2)	2.74(2)	2.82(2)	2.69(2)
O(25)	112.3(7)	1.71(1)	2.63(2)	2.81(2)	O(22)	112.2(7)	1.68(2)	2.67(2)	2.81(2)
O(13)	115.0(7)	101.7(7)	1.68(2)	2.66(2)	O(16)	116.4(7)	104.3(7)	1.70(1)	2.79(2)
O(32)	108.4(7)	109.4(7)	109.9(7)	1.73(2)	O(35)	106.0(7)	109.9(7)	108.0(7)	1.75(2)

Note. The As–O distances are underlined. The O–O distances are given above the diagonal, the O–As–O angles below.

octahedron than in the three others, as previously observed for the Fe(1)–O and Fe(2)–O distances in II-$Na_3Fe_2(AsO_4)_3$.

Oxygen windows. The radii R of the oxygen windows which separate neighboring Na sites were systematically examined (Table 9). Three kinds of windows must be taken into account:

(i) The windows which separate two neighboring Na(2*p*) positions belonging to different sextuplets. They are the widest ones: R = 2.38 Å for II-$Na_3Fe_2(AsO_4)_3$; the substitution of Al for Fe does not lead to significant variations in R, except for the O(16)O(14)O(26)O(24) window which separates Na(24) from the vacancy □(26): R = 2.48 Å.

(ii) Those that separate two Na(2p) neighboring positions belonging to the same sextuplet (R = 1.89 Å for II-$Na_3Fe_2(AsO_4)_3$). Three of them become very narrow (R < 1.85 Å) and the two widest ones are located in the vicinity of the vacancy □(26).

(iii) Those which separate the Na(1) site from the six neighboring Na(2p) sites: similarly, the widest one (R = 1.97 Å) separates Na(1) from the vacancy.

DISCUSSION

The present crystal structure determination of the *ordered* form α of $Na_3Al_2(AsO_4)_3$ enabled us to have a better understanding of the interactions between the mobile ions along the two possible conduction pathways which were proposed for the *disordered* form β of II-$Na_3Fe_2(AsO_4)_3$ (6).

The Na(24)–□(26) sequence in $Na_3Al_2(AsO_4)_3$ is common to both models of conduction paths (*a* and *b*) and, because of its large size, the oxygen window which sepa-

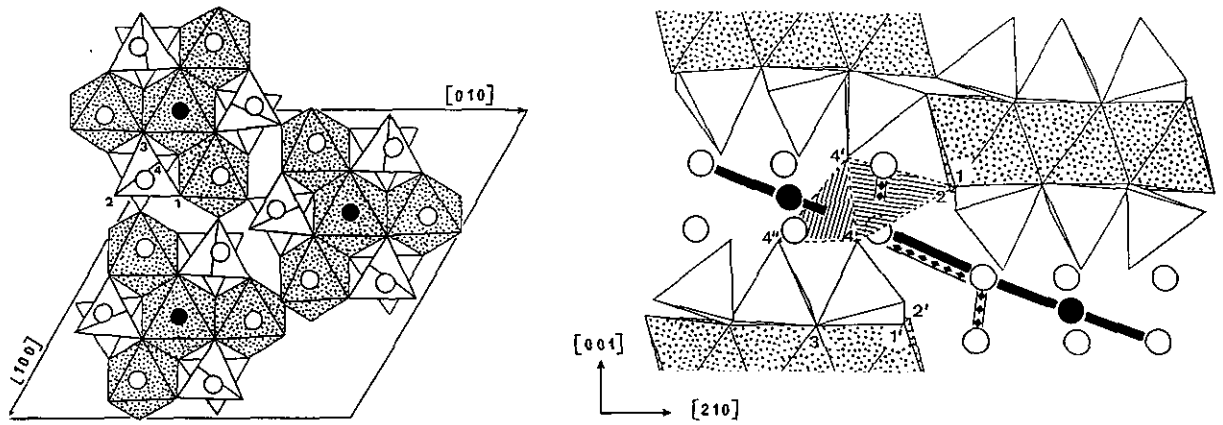

FIG. 3. Partial representations of the structure of II-$Na_3Fe_2(AsO_4)_3$ showing the arrangement of FeO_6 octahedra (shaded) and AsO_4 tetrahedra. The numbers refer to oxygen atoms. Filled circles: Na(1). Open circles: Na(2). Left, projection along [001]. Right, projection along [010]. The *a* and *b* models of conduction paths (*a* in black, *b* with lozenges) and two triangular oxygen windows are represented.

TABLE 8
Interatomic Distances (Å) and Angles (°) in AlO_6 Octahedra of α-$Na_3Al_2(AsO_4)_3$

Al(11)	O(32)	O(32)	O(33)	O(33)	O(31)	O(31)
O(32)	1.87(2)	2.68(3)	2.73(2)	2.59(2)	2.75(3)	3.79(2)
O(32)	91(1)	1.87(2)	2.59(2)	2.73(2)	3.79(2)	2.75(3)
O(33)	93.4(6)	87.3(6)	1.88(1)	3.75(3)	2.69(2)	2.65(2)
O(33)	87.3(6)	93.4(6)	179(1)	1.88(1)	2.65(2)	2.69(2)
O(31)	92.9(6)	175.4(8)	90.5(7)	88.7(7)	1.92(2)	2.54(3)
O(31)	175.4(8)	92.9(6)	88.7(7)	90.5(7)	83(1)	1.92(2)
Al(14)	O(34)	O(34)	O(36)	O(36)	O(35)	O(35)
O(34)	1.84(2)	2.51(3)	2.74(2)	2.68(2)	2.76(3)	3.75(2)
O(34)	86(1)	1.84(2)	2.68(2)	2.74(2)	3.75(2)	2.76(3)
O(36)	94.4(6)	91.7(7)	1.89(1)	3.77(3)	2.52(2)	2.71(2)
O(36)	91.7(7)	94.4(6)	172(1)	1.89(1)	2.71(2)	2.52(2)
O(35)	95.0(6)	177.2(8)	90.9(7)	83.0(6)	1.91(2)	2.57(3)
O(35)	177.2(8)	95.0(6)	83.0(6)	90.9(7)	84(1)	1.91(2)
Al(21)	O(21)	O(21)	O(11)	O(11)	O(31)	O(31)
O(21)	1.89(2)	2.81(2)	2.61(2)	2.92(2)	2.80(2)	3.86(2)
O(21)	96(1)	1.89(2)	2.92(2)	2.61(2)	3.86(2)	2.80(2)
O(11)	86.6(6)	100.4(6)	1.92(1)	3.82(3)	2.66(2)	2.68(2)
O(11)	100.4(6)	86.6(6)	170(1)	1.92(1)	2.68(2)	2.66(2)
O(31)	92.5(6)	169.4(7)	85.5(6)	86.4(6)	1.99(2)	2.54(3)
O(31)	169.4(7)	92.5(6)	86.4(6)	85.5(6)	79(1)	1.99(2)
Al(24)	O(24)	O(24)	O(14)	O(14)	O(34)	O(34)
O(24)	1.83(1)	2.91(2)	2.65(2)	2.79(2)	2.70(2)	3.81(2)
O(24)	105(1)	1.83(1)	2.79(2)	2.65(2)	3.81(2)	2.70(2)
O(14)	91.3(6)	97.4(6)	1.89(1)	3.74(3)	2.68(2)	2.57(2)
O(14)	97.4(6)	91.3(6)	166(1)	1.89(1)	2.57(2)	2.68(2)
O(34)	89.1(6)	164.7(7)	86.6(6)	82.2(6)	2.02(2)	2.51(3)
O(34)	164.7(7)	89.1(6)	82.2(6)	86.6(6)	77.8(9)	2.02(2)
Al(22)	O(12)	O(22)	O(23)	O(13)	O(32)	O(33)
O(12)	1.86(2)	2.62(2)	2.84(2)	3.74(2)	2.65(2)	2.62(2)
O(22)	89.3(7)	1.87(2)	2.90(2)	2.86(2)	2.69(2)	3.87(2)
O(23)	99.4(7)	102.0(7)	1.87(1)	2.58(2)	3.85(2)	2.78(2)
O(13)	169.0(8)	98.7(8)	86.3(6)	1.90(2)	2.66(2)	2.68(2)
O(32)	86.6(7)	87.9(7)	168.4(6)	86.2(7)	2.00(1)	2.73(1)
O(33)	84.6(7)	166.6(7)	90.8(6)	86.0(6)	79.8(6)	2.03(2)
Al(25)	O(26)	O(25)	O(16)	O(15)	O(36)	O(35)
O(26)	1.83(1)	2.87(2)	2.66(2)	2.80(2)	2.71(2)	3.80(2)
O(25)	101.0(7)	1.89(2)	2.87(2)	2.63(2)	3.83(2)	2.73(2)
O(16)	90.7(6)	98.2(8)	1.91(2)	3.81(2)	2.66(2)	2.61(2)
O(15)	97.2(7)	87.4(7)	169.4(7)	1.91(2)	2.64(2)	2.69(2)
O(36)	91.0(6)	166.9(7)	86.8(6)	85.9(7)	1.96(2)	2.52(2)
O(35)	168.9(6)	89.4(6)	83.9(7)	87.1(7)	79.1(61)	1.99(1)

Note. Al–O distances are underlined. O–O distances are given above the diagonal, O–Al–O angles below.

rates the Na(24) site from the □(26) vacancy is an easy passageway. The Na(24) ion is displaced of 0.55 Å toward the vacancy and displays the highest temperature factor (B_{eq} = 2.39(26) Å^2).

Along the *b*-pathway, both sodium sites Na(21) and Na(22) are displaced toward the vacancy □(26) while, along the *a*-pathway, the Na(1)–□(26) distance is slightly increased. This tends to indicate that the mobile ions are more likely to diffuse along the *b* model rather than the *a* model. The comparison of the temperature factors of the Na(1) and Na(2) sites in II-$Na_3Fe_2(AsO_4)_3$ (2.04 and 3.98 Å^2, respectively) favors this conclusion.

The phase transition from the disordered form β to the room-temperature form α of $Na_3Al_2(AsO_4)_3$ was previously shown (2) to be accompanied by an important decrease in the ionic conductivity (Fig. 1). In order to interpret this, we have examined how the *b* network of diffusion pathways is modified by the $\beta \rightarrow \alpha$ transition. One can reasonably suppose that the more narrow an oxygen window, the more difficult for a sodium ion to pass through it. If we consider the diffusion of a sodium ion to be improbable through the windows with $R \leq 1.84$ Å and eliminate these windows from the path-network, it appears that the diffusion through the remaining win-

TABLE 9
Na-Na Distances and Radii R of the Oxygen Windows (Å) in α-$Na_3Al_2(AsO_4)_3$

Na sites	Distances (a)	(b)	Oxygen windows	R (Å)
	Na(2p)–Na(2p) pairs belonging to different sextuplets			
Na(22)–Na(22)	3.09(2)	3.04	O(12)–O(12)–O(22)–O(22)	2.40
Na(25)–Na(25)	3.22(2)	3.04	O(15)–O(15)–O(25)–O(25)	2.35
Na(21)–Na(23)	3.25(1)	3.05	O(11)–O(13)–O(21)–O(23)	2.37
Na(24)–□(26)	2.50(1)	3.05	O(16)–O(14)–O(26)–O(24)	2.48
	Na(2p)–Na(2p) pairs belonging to the same sextuplet			
Na(21)–Na(25)	3.49(1)	3.43	O(13)–O(46)–O(41)	1.838
Na(25)–Na(23)	3.51(1)	3.45	O(15)–O(41)–O(45)	1.841
Na(23)–Na(24)	3.83(2)	3.40	O(11)–O(45)–O(43)	1.902
Na(24)–Na(22)	3.47(1)	3.43	O(16)–O(43)–O(44)	1.772
Na(22)–□(26)	3.33	3.45	O(12)–O(44)–O(42)	1.913
□(26)–Na(21)	3.15	3.40	O(14)–O(42)–O(46)	1.916
		Na(1)–Na(2p) pairs		
Na(1)–Na(25)	3.03(1)	3.05	O(46)–O(41)–O(45)	1.820
Na(1)–Na(23)	3.11(1)	3.03	O(41)–O(45)–O(43)	1.893
Na(1)–Na(24)	3.47(2)	3.07	O(45)–O(43)–O(44)	1.862
Na(1)–Na(22)	2.96(1)	3.05	O(43)–O(44)–O(42)	1.880
Na(1)–□(26)	3.15	3.03	O(44)–O(42)–O(46)	1.975
Na(1)–Na(21)	2.97(2)	3.07	O(42)–O(46)–O(41)	1.848

Note. (a) calculated from the coordinates refined in the space group $C2$; (b) calculated from the coordinates of the Na sites in II-$Na_3Fe_2(AsO_4)_3$.

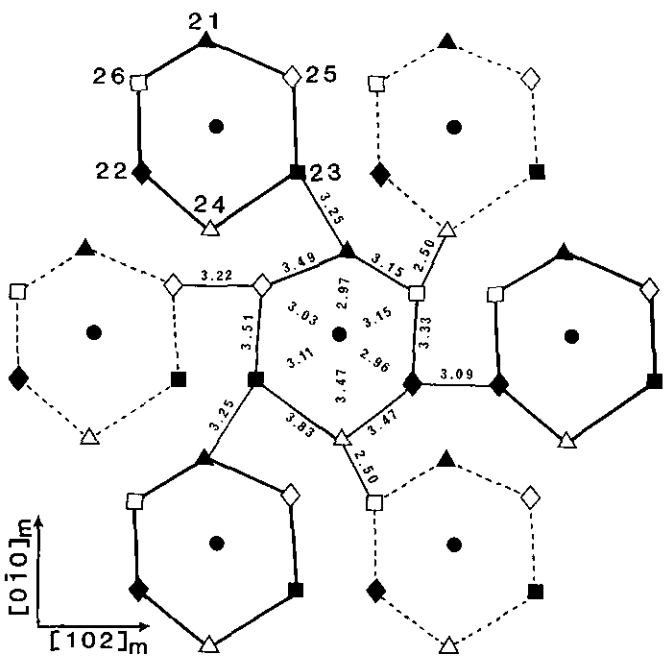

FIG. 4. Arrangement of the sodium sites in the structure of α-$Na_3Al_2(AsO_4)_3$ (space-group C2). Projection along $[001]_h = [10\bar{1}]_m$. The sites are represented by graphical symbols and the corresponding numbers are given at the top left of the figure. Distances between the sodium sites are given in Å. The lines drawn between the sites represent the conduction paths according to the b model proposed for the β form. The average z_h coordinates of the sodium sextuplets are about 0, $-1/6$, and $+1/6$, for the central sextuplet, the three ones with dotted lines and the three others, respectively.

dows ($R \geq 1.90$ Å, see Table 9), is restricted along pathways with $[001]_m$ as the general direction (12). The loss of symmetry associated with the $\beta \rightarrow \alpha$ transition would therefore be accompanied by a loss of the three-dimensional character of the conduction.

REFERENCES

1. H. Schwarz and L. Schmidt, *Z. Anorg. Allg. Chem.* **387,** 31 (1972).
2. F. d'Yvoire, M. Pintard-Scrépel, and E. Bretey, *Solid State Ionics* **18–19,** 502 (1986).
3. F. d'Yvoire, M. Pintard-Scrépel, E. Bretey, and M. de la Rochère, *Solid State Ionics,* **9–10,** 851 (1983).
4. M. de la Rochère, F. d'Yvoire, G. Collin, R. Comès, and J.-P. Boilot, *Solid State Ionics* **9–10,** 825 (1983).
5. C. Delmas, J.-C. Viala, R. Olazcuaga, G. Le Flem, P. Hagenmuller, F. Cherkaoui, and R. Brochu, *Solid State Ionics* **3–4,** 209 (1981).
6. F. d'Yvoire, E. Bretey, and G. Collin, *Solid State Ionics* **28–30,** 1259 (1988).
7. F. d'Yvoire, *Bull. Soc. Chim.* 1237 (1962).
8. A. Modaressi, A. Courtois, R. Gerardin, B. Malaman, and C. Gleitzer, *J. Solid State Chem.* **40,** 301 (1981).
9. B. Malaman, M. Ijjaali, R. Gerardin, G. Venturini, and C. Gleitzer, *Eur. J. Solid State Inorg. Chem.* **29,** 1269 (1992).
10. C. Masquelier, F. d'Yvoire, and N. Rodier, *J. Solid State Chem.* **95,** 156 (1991).
11. "International Tables for X-Ray Crystallography," Vol. IV, Kynoch, Birmingham, 1974.
12. C. Masquelier, F. d'Yvoire, and G. Collin, "Solid State Ionic Materials" (B. V. R. Chowdari, M. Yahaya, I. B. Talib, and M. M. Salleh, Eds.), p. 167. World Scientific, Singapore, 1994.